

# STRUCTURAL DESIGN, DEVELOPMENT AND TESTING OF A SMALL EXPERIMENTAL SATELLITE: SATEX-1

R. Peralta, Y. Fairuzov, M. Navarrete, J. Aguirre\* F. Serranía.

Lab. Ing. Aeroespacial, Instituto de Ingeniería-UNAM, \*Instituto de Investigaciones Eléctricas.  
Apartado Postal 70-472, Coyoacán 04510, México, D. F., Fax: 622 89 46

## Abstract

A 50 kg. satellite is being developed at the University of Mexico as an engineering test bed. SATEX-1 is programmed to be launched to polar orbit early in 1995 by Ariane.

The satellite structure comprises aluminum sandwich panels and composites in the form of a cube made with two matting U-shaped parts. This solution was selected for simplicity during assembly and testing. The s/c body is further stiffened by an internal panel which supports a pressurized gas tank and other hardware. All panels are joined by standard corner and edge close-outs and splices.

At present, a finite element model for the validation of the design, regarding static and dynamic behaviour is being conducted. The paper presents numerical results for quasistatic and dynamic analysis, such as eigen-values, free vibration and sinusoidal vibrations.

The testing program follows closely launcher agency requirements and is supported by previous similar experiences in our laboratory. Also, a general description of the project is included.

## 1. Introduction

Spacecraft design and development requires a demanding level of engineering, usually associated with most modern methods. Moreover, in a research institute environment, it can provide training, with multiplicative potential applicable in broad fields with urgent and practical need of such quality. This is the central objective of this project as seen from a country in technological development, Ref. 1.

This communications satellite is the first in series of satellites to experiment with the performance of a general bus, since most any payload requires the presence of communication, Ref. 1. Three different radio frequency and optical links provide redundancy, but the motivation is to characterize future bands with respect to signal degradation under meaningful tropical rain conditions by means of a mobile receptor-laboratory. Otherwise, we follow a

standard design, that is conceived to provide some detailed knowledge of new advances in aerospace technology, and bring them to a more general practice, Ref. 3-11.

Flight qualification tests will be carried out according to standardized procedures, following the instructions for the ASAP platform on board an Ariane launched to polar orbit, Ref. 12. As required, the structure is being designed to survive launch and protect the internal hardware, but it's main function is during ascent to ensure complete passivity. The general view of the SATEX-1 satellite is shown in Fig. 1.

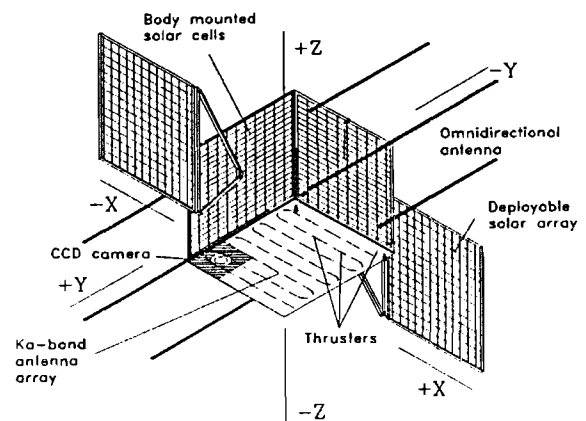


Fig. 1 SATEX-1 general view

## 2. Structural analysis of the main body

### 2.1. Satellite main structure

The main structure of the satellite consists of two U-shaped parts, as shown in Fig. 2. The structure was selected in order to simplify the assembling process and to facilitate access to any subsystem during testing and integration. When joined together, these two structures form a cube of 450 x 450 x 450 mm size. The body of the spacecraft is additionally stiffened by means of an

internal panel, which supports the pressurized gas tank and other hardware.

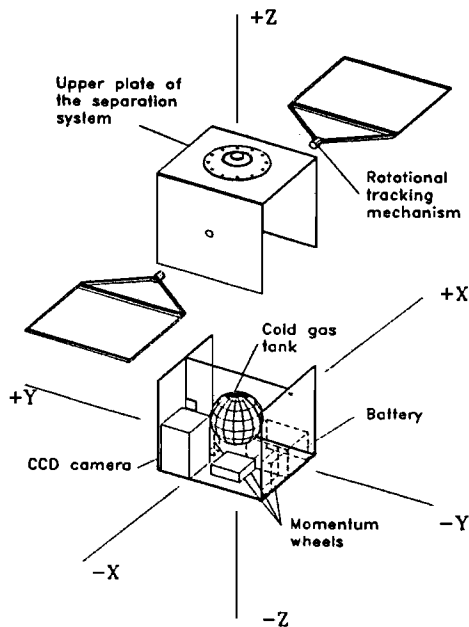


Fig. 2 SATEX-1 exploded view

The main body will be formed using sandwich panels that comprise two skins of aluminum 2024-T3 of 0.8 mm thickness and a core of aluminum 5066 hexagonal honeycomb of 5mm thickness (distance between the skins). All panels will be joined by standard corner and edge close-outs and splices.

The SATEX-1 will be mounted on the launch vehicle using the standard separation system normally utilized by auxiliary payloads in Arianespace, Ref. 12. The attachment will be made with 12 bolts located on a diameter of 248mm.

## 2.2. Mechanical environment

During the flight, the satellite is subjected to static and dynamic loads induced by the launch vehicle. Dimensions and design of the spacecraft primary structure must therefore allow for the most severe load combination that can be encountered at a given instant of flight.

From the point of view of static loads, conditions are critical at the following times, Ref. 13:

- during maximum dynamic pressure.
- just before thrust termination.
- during thrust tail off.

The quasi-static accelerations at the center of the mass of the spacecraft for Ariane launch vehicle, are given in Table 1, Ref. 14.

Table 1

Ariane's limit accelerations

	Accelerations (g's)	
Flight event	Axial axis	Lateral axis
Maximum dynamic pressure	-3.5	± 2
Second stage burnout	-7.9 +3.2	± 1

The dynamic environment includes:

- Low frequency longitudinal vibrations. The vibration level at the base of the payload is  $\leq 1.25g$  from 6 to 100 Hz. This spectrum takes into account any sinusoidal or transient vibrations in this band-width.
- Low frequency lateral vibrations. The vibration level at the base of the payload is  $\leq 0.8 g$  from 5 to 18 Hz and  $\leq 0.6 g$  from 18 to 100 Hz.
- Random vibration.
- Acoustic vibrations. Acoustic vibrations are generated by engine noise, buffeting and boundary-layer noise.
- Shocks. The satellite is subjected to shocks during separation of the fairing, during separation of main passenger and during actual spacecraft separation.

Due to the very nature of the launch conditions a finite element analysis has been performed in order to validate the design.

## 2.3. Finite element model of the main structure

The finite element model used to simulate the main structure is shown in Fig.3. The panels of the satellite were modelled by the 3-D laminated sandwich shell elements, Ref. 15.

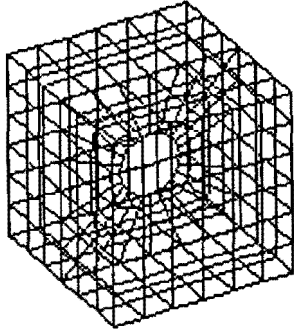


Fig. 3 Finite element model of the satellite main structure

The inertia properties of the components of the payload and subsystems attached to the panels, were described by concentrated mass elements.

The boundary conditions were imposed according to the mounting conditions of the spacecraft to the platform. The final element model of the main structure consists of 414 nodes, 188 laminated sandwich shell elements and 108 concentrated mass elements.

#### 2.4. Static analysis

The satellite is exposed to linear accelerations during launch, causing tension and compression of the structure in the longitudinal and lateral directions.

The maximum linear acceleration according to the acceleration profile of Ariane 4, occurs when the second stage burnout takes place and is of the order of  $42 \text{ m/s}^2$ . Taking into account low frequency vibrations, the resulting acceleration of  $68.7 \text{ m/s}^2$  was used for the quasi-static analysis. The lateral acceleration is negligible and was therefore not taken into account.

This quasi-static analysis includes the calculation of stresses, forces and reactions. Due to the configuration of the sandwich structure, calculations are given for three different components namely, outside skin, core and inside skin.

Table 2 shows a summary of the maximum stresses indicating different values for the inside and outside skins as well as the core, computed for the material principal directions.

Table 2

Maximum stresses of sandwich structure

	Outside skin	Core	Inside skin
$\sigma_{xx}$ , Pa	$-3.33 \times 10^6$	-	$3.72 \times 10^6$
$\sigma_{yy}$ , Pa	$-6.675 \times 10^6$	-	$-6.41 \times 10^6$
$\tau_{xy}$ , Pa	$-1.137 \times 10^6$	-	$-1.207 \times 10^6$
$\tau_{xz}$ , Pa	-	$1.34 \cdot 10^3$	-
$\tau_{yz}$ , Pa	-	$2.24 \cdot 10^3$	-

Fig. 4 shows the inside skin distribution of normal stresses  $\sigma_{xx}$  due to the linear acceleration in each face of the structure. Fig. 5 shows the outside skin distribution of normal stresses  $\sigma_{xx}$  in each face of the structure. Fig. 6 shows the core shear stresses  $\tau_{xz}$  in each face of the structure.

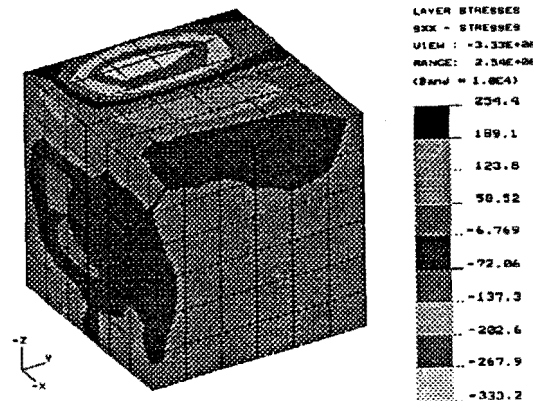


Fig. 4 Distribution of normal stress in the inside skin

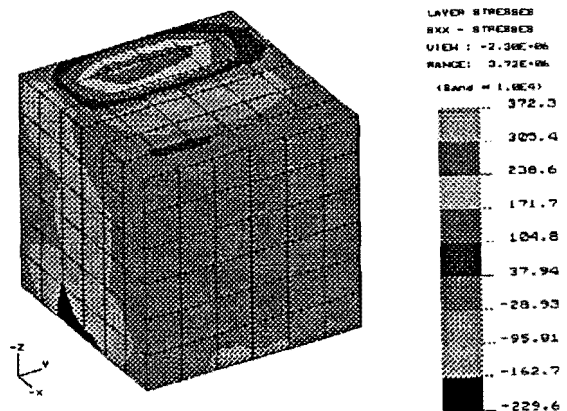


Fig. 5 Distribution of normal stress in the outside skin

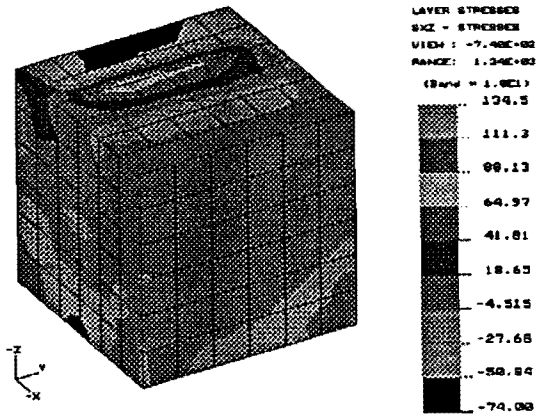


Fig. 6 Distribution of transverse shear stress in the core

Observing Fig.4 and Fig. 5 it may be noticed that the maximum stresses are present on the face of the satellite where the maximum weight is concentrated (-Z face), and according to Table 2 the maximum stresses are generated in the outside skin of this face.

Another important remark is that the permissible stresses for aluminium sandwich panels (skin and core separately) given by the manufacturer, Ref. 16, are two orders of magnitude smaller than the presently calculated stresses. Therefore, it is valid to state that the structure has more than enough resistance to withstand static loads. Nevertheless, further analysis will show that the mechanical properties of the panels had to be determined taking into account dynamic loads.

## 2.5. Dynamic analysis

### 2.5.1. Eigenvalue analysis

To avoid dynamic coupling between the low frequency vehicle and spacecraft modes, the spacecraft must be designed with a structural stiffness which ensures that the fundamental frequency of the spacecraft in the thrust axis is higher than 100 Hz, and that the fundamental frequencies of the spacecraft in the lateral axes are higher than 50 Hz. In order to determine the natural frequencies of the satellite, an eigenvalue analysis was performed.

The calculated values of fundamental frequencies in longitudinal and lateral directions are shown in Table 3.

Table 3

Spacecraft fundamental frequencies.

Direction	Frequency, Hz
Z	182
X	84
Y	120

The fundamental mode for longitudinal directions is shown in Fig. 7. As it may be observed the fundamental frequencies are sufficiently high to avoid dynamic coupling between the Ariane 4 and the satellite.

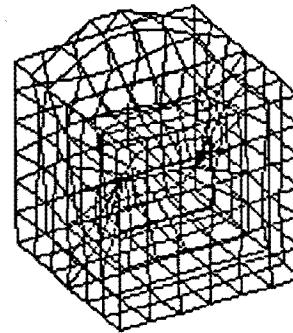


Fig. 7 Fundamental mode in the thrust axis

### 2.5.2. Frequency response analysis

The steady state response of the structure to base excitation was evaluated using frequency response analysis. The base motion was described by the spectra given by Arianespace for sinusoidal and vibration tests (see Table 4).

Table 4

Base spectra of Ariane 4

	Frequency range, Hz	Amplitude
Longitudinal	5-6	17.3 mm
	6-35	3.75 g
	35-100	2.5 g
Lateral	5-100	1.0 g

For the calculations of the frequency response spectra, 50 first lowest modes were used. The viscous damping factor was assumed to be equal to

10%. The amplitude response spectra for displacements and accelerations in the longitudinal direction is shown in Fig. 8 and Fig. 9 respectively.

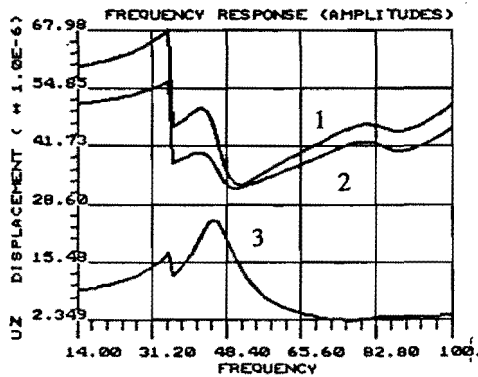


Fig. 8 Response amplitude spectrum for the displacement in the launch direction  
1-Node 298; 2-Node 292; 3-177

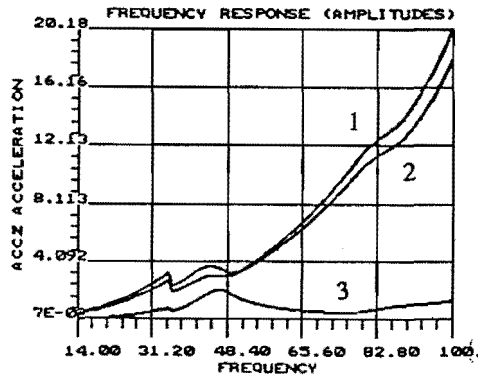


Fig. 9 Response amplitude spectrum for acceleration in launch direction  
1-Node 298; 2-Node 292; 3-Node 172

Fig. 8 shows the nodes with the highest amplitude (nodes 292 and 298); these nodes coincide with the location of the centroid of the battery box (the heaviest of all the components in the satellite). In the same figure, node 177 represents a typical vibration of a CCD camera. It should be note that all the results presented here show relative motion of the structure with respect to the base.

Fig. 10 represents the response spectra for lateral acceleration (x-direction) caused by lateral vibrations of the base. The absence of high peak values determines that the vibrations in the three directions do not cause damage to the structure.

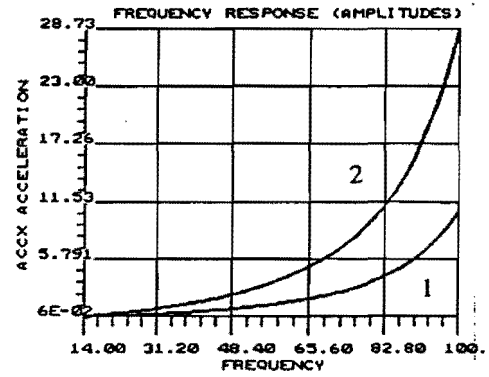


Fig. 10 Response amplitude spectrum for acceleration in X direction  
1-Node 171; 2-333

Further experimental tests of an engineering prototype will be performed in order to assess the numerical results presented in this paper. The experimental results are also required for qualification and acceptance of the SATEX-1 by the launch agency.

### 3. Conclusions

1. Numerical results presented in this paper show that the preliminary design of the satellite is capable of withstanding static and dynamic loading.
2. The structural analysis shows that the mechanical properties of materials used and the sizing of the structure have to be determined taking into account mainly dynamic loads.
3. The results show that use of sandwich panels allows for a high stiffness -to-weight ratio.
4. The frequency analysis presented will allow the choice of preferable locations for equipment sensitive to vibrations.

### References.

1. Peralta-Fabi R. et al., "Viabilidad de un Satélite Latinoamericano de Percepción Remota" *Inst. do Pesquisas Espaciais/INPE-Brasil* Gramado, Brasil, 1986.
2. Peralta-Fabi R., et al., "El Programa de Satélites Experimentales de México" *II Simposio Latinoamericano de Percepción Remota IGA-SELPER-SCF*. Bogotá, Colombia, 1987.
3. Peralta-Fabi R., et al., "Experimental Satellite Series (SATEX): A development effort of several research institutions in Mexico" *XXVIII Committee on*

*Space Research COSPAR*. The Hage, Netherlands, 1990.

4. Peralta-Fabi, R., et al., "Bus development for the multitask engineering test satellite:SATEX", Proc. of O.E: Aerospace Science and Sensing 1993, Orlando, Florida, USA, 1993

5. Peralta-Fabi R., et al., "El diseño y desarrollo de satélites experimentales mexicanos" V *Simposio Latinoamericano de Percepción remota. SELPER*. Cusco, Perú, 1991.

6. Fouquet, M., "The UoSAT-5 Earth Imaging System-In-Orbit Results" *Proc. of Small Satellite Technologies and Applications II*. Ed. B. J. Horais, SPIE, Vol. 1691, Orlando, Florida, USA 1992.

7. Bonsall, C.A.and R. G. Moore "NUSAT-1-The First Ejectable Getaway Special" *Proc. of 1985 Get Away Special Experimenter's Symposium*. pp 87-99. NASA, GSFC, Greenbelt, Maryland. October 1985.

8. Defense Systems Inc. "The GLOMR SATELLITE PAYLOAD G-308" *Proc. of 1985 Get Away Special Experimenter's Symposium*. pp 285-291 NASA, GSFC, Greenbelt, Maryland. October 1985.

9. Bonsall, C:A:, "NUSAT Update" *Proc. of 1986 Get Away Special Experimenter's Symposium*. pp 63-69 NASA, GSFC, Greenberlt, Maryland, October 1986.

10. Megill, L. R., "GS-100 & GS-200 Two Commercial light Satellites". *AIAA/DARPA Meeting on Lightweight Satellite Systems*. pp 225-229 Monterey, California. August 1987.

11. Rosengren, M., "ERS-1- An Earth Observer that Exactly Follow Its Chosen Path", *ESA Bulletin* No. 72, 1992, pp 76-82

12. Ariane 4, "Ariane Structure for Auxiliary payload (ASAP), *User's Manual, Arianespace*, Issue 2-Rev.

13. Griffin, M. D. James, R. F. "Space vehicle design" *American Institute of Aeronautics and Astronautics, Inc*. Washington, D.C., 1991.

14. Agrawal, B. N. "Design of geosynchronous spacecraft " *Prentice Hall, Inc*. Englewood Cliffs, 1986.

15. NISA II- DISPLAY II. *User's Manual, Center for Engineering and Computer Technology, Engineering Mechanics Research Corporation (EMRC)*, Michigan, USA, 1990.

16. Data sheets, Hexel Honeycomb TSB 124, Bonded Honeycomb Sandwich Construction, 1989, pp 6-7, 28